WAFER-SCALE ENCAPSULATED SAW TEMPERATURE AND PRESSURE SENSORS FOR HARSH ENVIRONMENTS

Eldwin J. Ng[1], Jaibir Sharma[1], Eva Wai Leong Ching[1], Guoqiang Wu[1],
Didier Pohl[2] and Olivier Vancauwenberghe[2]
[1]Institute of Microelectronics, Singapore and
[2]Safran Tech, Safran Sensing Systems, Paris-Saclay, France

ABSTRACT

Passive SAW sensors do not require circuitry or power and are ideal for harsh environments or rotating machinery. AlN-based thin film SAW resonators for temperature and pressure sensors have been developed in this work using AlGe wafer-scale encapsulation for device protection, pressure reference, high stability, and small size. Temperature and pressure co-testing of both sensors up to 160°C and 60 bar revealed ~1% full-scale accuracy.

KEYWORDS

Surface Acoustic Wave (SAW), Temperature Sensors, Pressure Sensors, Wafer-scale Encapsulation

INTRODUCTION

SAW devices are commonly used for providing stable frequency references for wireless communications, but have also been demonstrated for wirelessly interrogated passive temperature [1] and pressure sensors [2-5] without requiring batteries or circuitry. They are thus well suited for harsh environments or for placement on rotating machinery. Such sensors have numerous applications in the aerospace or oil and gas industries. AlN is known to be a stable piezoelectric material that remains operational at high temperatures [6]. AlN-based SAW temperature and pressure sensors have been previously demonstrated [7, 8]. The approach in this work discusses the wafer-scale encapsulation of such AlN SAW sensors using AlGe wafer bonding. AlGe wafer bonding has been demonstrated to be stable at 300°C [9], and is thus a viable candidate for encapsulation. Wafer-scale encapsulation by bonding a cap wafer over a SAW wafer provides several key benefits for this sensor device, such as to:

a) Protect the SAW device against contaminants and oxidation for stability. The surface acoustic wave propagates on the front surface protected by the encapsulation. Fluids or residue on the back surface of the membrane do not directly affect the resonance.
b) Provide a reference vacuum cavity for accurate measurement of pressure.
c) Eliminate the need to seal around the pressure port to the package with die attach, as the die attach typically cannot sustain high pressures and/or temperatures. This also has the added effect of reducing frequency drift due to changing package stresses.
d) Enable a small, low-profile form factor, with batch fabrication at low cost.

DESIGN

Structure

AlN-on-silicon SAW resonators were designed around the 440 MHz amateur radio band for wireless communication frequency compatibility and good wireless communication range. Two SAW resonators were designed on the same chip with slightly different frequencies, one for temperature sensing, and the other for pressure sensing (Figure 1). Split interdigitated transducer (IDTs) SAW designs were applied [7]. While simultaneous measurement of the dual sensor configuration allows for cross-compensation, it is still necessary to design higher accuracy pressure sensors that are relatively insensitive to temperature and vice versa. The SAW temperature sensor in this work consists of a piezoelectric stack (Mo/AlN/Mo) on top of a silicon substrate, and is expected to have a TCf of around -25 to -30 ppm/°C. The SAW pressure sensor, on the other hand, includes an additional layer of silicon oxide between the piezoelectric stack and the silicon substrate for the purpose of temperature compensation [8]. It is designed to be on a membrane with a back port for increased pressure sensitivity. An applied static pressure to the back port generates a stress on the SAW pressure sensor on the front side of the membrane and causes a shift in the resonant frequency. The key design parameters of the SAW sensors are listed in Table 1.

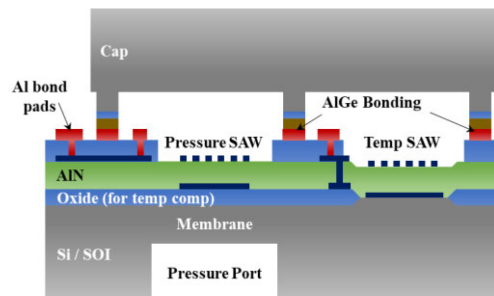

Figure 1. Encapsulated SAW pressure and temperatures sensors adjacent to each other on a single die.

Table 1. Design parameters of the SAW temperature and pressure sensors.

Design Parameters	Temperature Sensor	Pressure Sensor
Period (um)	9.8	9.2
Silicon oxide thickness (um)	None	0.7
Resonant Frequency (MHz)	457.5	437.5
Number of IDT pairs	60	60
Number of reflectors on each side	160	160
Pressure port diameter (mm)	None	1.0

Modelling

Since this SAW utilizes a composite stack of materials,

the device was modelled using finite element analysis. The TCf can be estimated using literature values of the material properties for silicon [10], oxide [11], and molybdenum [12]. Eigenmodes of a periodic structure of the IDT was modelled in COMSOL at various temperatures, accounting for the temperature-varying material properties as well as thermal expansion. The frequencies were extracted from the mode shapes and the simulated TCf is plotted for various oxide thicknesses (Figure 2). The temperature sensor does not have an oxide layer for maximum temperature sensitivity, while the pressure sensor has an optimum thickness of around 0.6-0.7 um for temperature compensation.

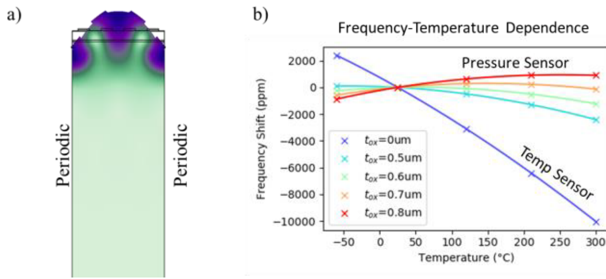

Figure 2. (a) Periodic simulation of the mode shape for TCf determination of the composite SAW, and (b) simulated frequency-temperature dependence of the SAW with different oxide thicknesses (normalized around 25°C).

To evaluate the full frequency response, 3D models of the full device were constructed. To allow for a reasonable computation time, quarter symmetry/anti-symmetry was applied, while maintaining a fine mesh (~λ/8 quadratic elements) in the SAW propagation direction for accurately capturing the main mode. The mesh size parallel to the IDT fingers was designed to be coarser, with the mesh size seen to affect the simulation accuracy of the transverse spurious modes. A model with 8 elements was seen to be reasonable for capturing some of the transverse modes while allowing for a reasonable simulation time of several hours for a full 3D model frequency sweep on a modern multicore workstation. The simulated transmission frequency sweeps are shown in Figure 3.

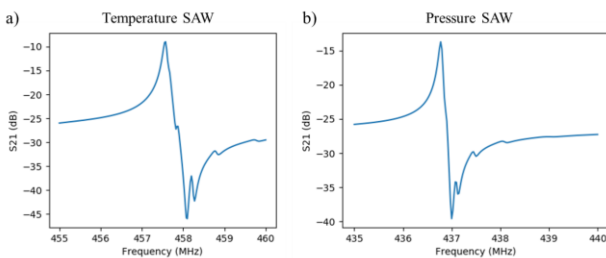

Figure 3. Simulated S21 frequency sweeps for (a) the temperature sensor, and (b) the pressure sensor.

To simulate the pressure coefficient of frequency (PCf), the substrate (with a port for the pressure sensor) and the cap were added to the model, and a prestressed condition was used, where a static pressure was applied on the back surface of the membrane against a fixed cap. The stresses in the stationary analysis were then used in the subsequent eigen analysis. From the stationary stress analysis, it is apparent that the stresses at the center and edges of the membrane are opposite – this is the guiding principle for the co-optimization of the cavity and the SAW dimensions, as the SAW resonance for the pressure sensor should be confined to a single region (either tensile or compressive) to avoid cancellation of the pressure-induced frequency shift (Figure 4). The simulated effect of pressure on the resonant frequency is shown in Figure 5.

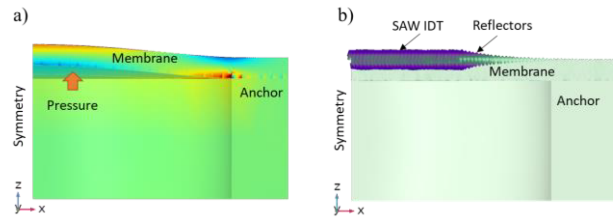

Figure 4. Simulated cross-section: (a) x-direction stress on the membrane with pressure applied from the back of the membrane: tensile (red) in the middle, and compressive (blue) at the edge; (b) SAW mode shape, confined largely to the center portion of the membrane.

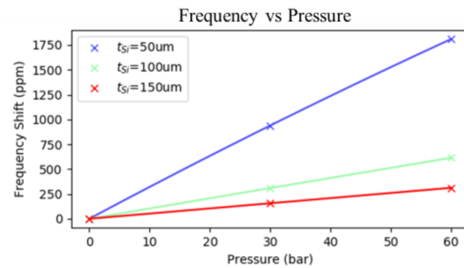

Figure 5. Simulated frequency-pressure dependence of the SAW pressure sensor, as a function of the silicon membrane thickness t_{si}.

FABRICATION

Wafer Fabrication

The fabrication of the device is shown in Figure 6, and starts with a silicon wafer or a Silicon-On-Insulator (SOI) wafer, which can be easily micromachined to form a port/membrane. A LOCal Oxidation of Silicon (LOCOS) process is then used to create regions of silicon oxide (0.7 um thick) for temperature compensation of the pressure sensor, while the temperature sensor is fabricated directly on the silicon regions. A bottom electrode of 0.2 um Mo is deposited and patterned, followed by a 1 um sputtered AlN layer. Vias through the AlN are etched and a top electrode of 0.2 um Mo is deposited and patterned with the SAW IDT and reflector designs. Silicon oxide (~2 um) is then deposited over the structure for electrical isolation, followed by a via etch. Al is then deposited and patterned for the seal ring, electrical routing, as well as bond pads.

Separately, a cap wafer with Ge / SiO_2 on a silicon substrate was etched for bonding to the SAW wafer, forming a seal ring around the SAW device. These wafers were bonded together, followed by thinning of the SAW wafer and etching a port for the pressure sensor. Partial dicing was used to reveal the bond pads, followed by singulation of the dies. The final device was <1 mm thick, with a die size of 4.5 x 3 mm. A scanning electron

microscope (SEM) cross-section image of the pressure sensor with a silicon membrane is as shown in Figure 7.

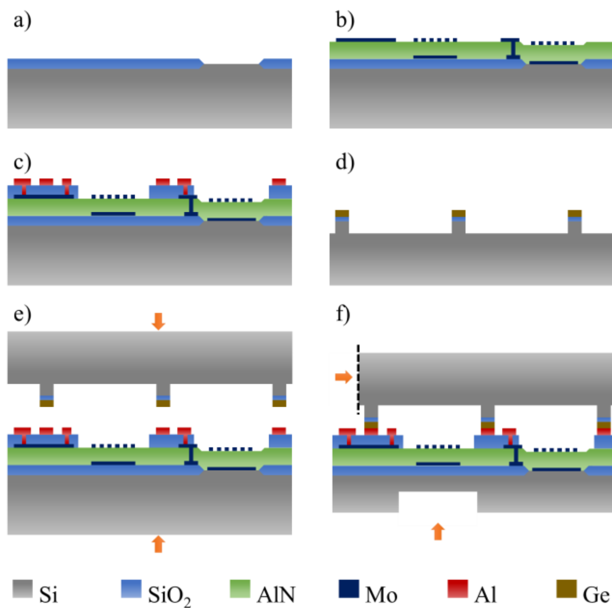

Figure 6. Fabrication process flow of the SAW pressure sensor: a) LOCOS for creating regions of silicon oxide and silicon, b) deposition and patterning of each layer of the Mo/AlN/Mo piezoelectric stack, c) formation of the electrical isolation and Al routing layers, d) cap wafer with Ge/SiO2 on Si, patterned through, e) bonding of the cap and SAW wafers, f) thinning of SAW wafer, back port etch, and partial dicing to expose the bond pads. The die are singulated after this by dicing fully through both wafers.

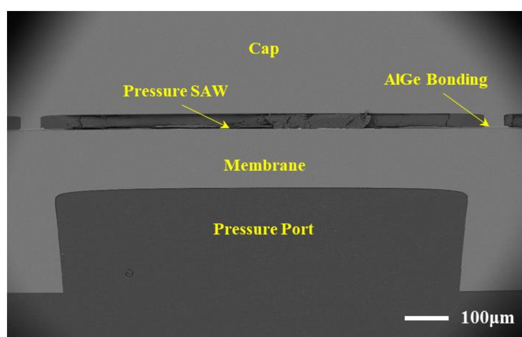

Figure 7. Cross-section SEM image of the pressure SAW sensor.

Packaging

The wafer-scale encapsulated die was attached with epoxy to a transistor outline (TO) header with a pressure pipe for pressure characterization. The epoxy die attach was applied at one end of the die (with the wire bond pads) and the rest of the die was suspended to reduce package stress drift on the SAW resonators (Figure 8). Wire bonds were then used to connect the device to the leads on the TO header. Finally, a cap was laser welded onto the TO header so that high fluid pressure could be applied hydrostatically around the die, including the membrane at the back of the die. The fluid also enters the pressure port at the back of the die and applies a pressure to the membrane pressure sensor.

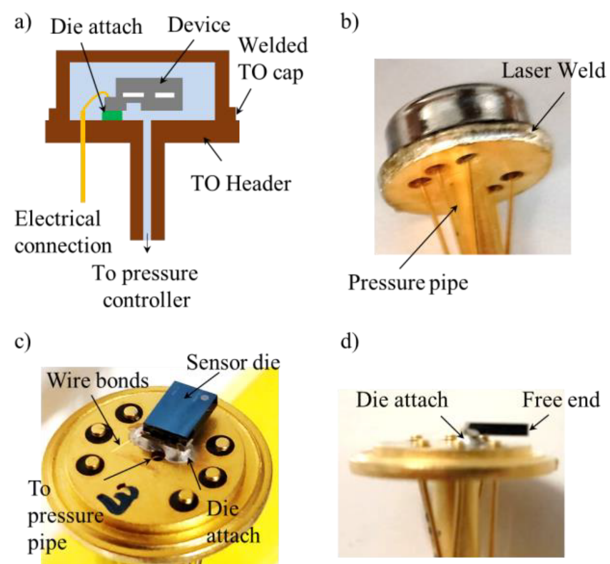

Figure 8. Packaging of sensor for high pressure characterization: a) Packaging concept, b) Welding seam of cap attached to TO header, c) die assembled on a TO header, d) side view of the suspended sensor die on a TO header.

CHARACTERIZATION

Wafer Probing

Probe station characterization of the devices with a network analyzer was performed across the temperature range from -60°C to 240°C, with the transmission measurement frequency sweeps for the temperature and pressure sensors shown in Figure 9. These were performed on the wafer-level for a SAW wafer with just the piezoelectric stack without encapsulation. For these measurements, the bottom electrode was grounded and each side of the IDT connected to separate ports of the network analyzer. The frequency of the temperature sensor is seen to shift noticeably more than that of the pressure sensor across temperature, due to the oxide compensation.

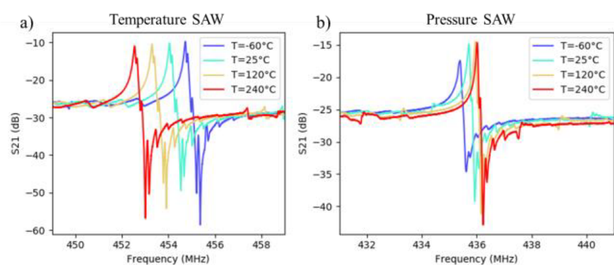

Figure 9. S21 measurement of the (a) temperature and (b) pressure SAW sensors.

Temperature and Pressure Co-testing

For high pressure characterization, the encapsulated devices were packaged as described in the previous section, followed by soldering to a PCB and electrically connected with coaxial cables. The pressure was applied by a hydraulic pressure calibrator connected to the pipe of the TO package and immersed into a silicone oil bath for temperature control. The temperature was swept from 30°C to 160°C and back to 30°C; for each temperature point, the

applied (gauge) pressure was swept from 0 bar to 60 bar and back to 0 bar. The resonant frequencies of both temperature and pressure SAW sensors were recorded and plotted against the temperature and pressure set points (Figure 10). The first and second order TCfs and PCfs are reported in Table 2. The accuracy observed was ~1% – the up and down sweep points hence are overlaid in the plot.

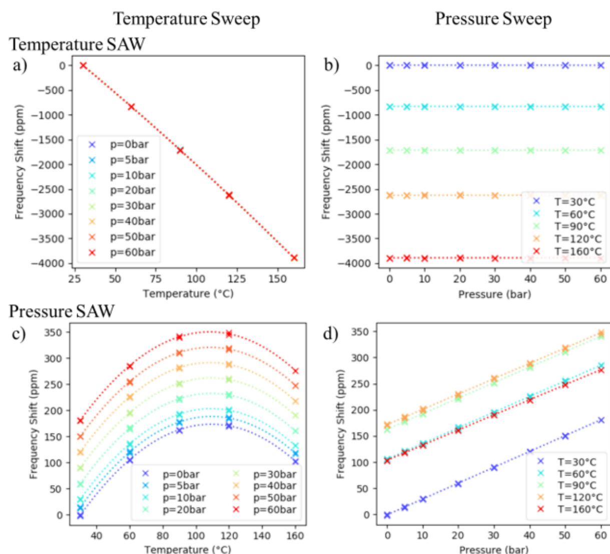

Figure 10. Temperature and pressure co-testing results for the temperature and pressure SAW sensors.

Table 2. Measured temperature sensitivities (around 25°C) and pressure sensitivities of the SAW resonators.

	Temperature Sensor	Pressure Sensor
TCf_1 (ppm/°C)	-27.2	+4.6
TCf_2 (ppb/°C^2)	-20	-27
PCf (ppm/bar)	0.0	+3.0

DISCUSSION

The SAW device performance is seen to match the simulations in terms of frequency and TCf. Spurious modes have been captured in the finite element model and may be reduced by future tuning the design of the SAW device.

Higher temperature co-testing requires several components to be modified – there are limitations in the packaging, connectors, cables, solder, as well as the hydraulic pressure and temperature bath fluids. Further development is required to extend the measurement range.

The measured pressure coefficient of frequency is seen to be rather low at ~3 ppm/bar. This was primarily due to the poor time etch control over the membrane thickness, resulting in the membrane being significantly thicker than planned (~140 um). This may be improved using an SOI wafer, but further study is needed to ensure that any notching effects at the silicon-oxide interface do not present the risk of crack propagation. Even accounting for the membrane thickness, there is still ~40% PCf discrepancy observed between the model (Figure 5) and measurement that needs to be resolved.

With the dual temperature and pressure sensors, the cross-sensitivity, especially of the pressure sensor to temperature, may also be calibrated away to obtain accurate pressure measurements

Finally, wireless characterization of the device needs to be performed for a system-level characterization. The SAW frequency may also need to be further fine-tuned or trimmed to fit within the allowed radio frequency bands.

CONCLUSION

AlN-based composite SAW resonators were fabricated for use in wireless temperature and pressure sensors for harsh environments. AlGe wafer-scale encapsulation of the sensors allowed for stable, low-profile sensors. Temperature compensation of the pressure sensor was achieved using a thin silicon oxide layer below the piezoelectric, and temperature and pressure co-testing revealed stable devices up to 160°C and 60 bar.

REFERENCES

[1] Alfred Pohl, G. Ostermayer, and F. Seifer, "Wireless Sensing Using Oscillator Circuits Locked to Remote High-Q SAW Resonators," *IEEE Trans. Ult. Ferr. Freq. Ctrl.,* vol. 45, no. 5, pp. 1161-1168, 1998.

[2] T. Baron *et al.*, "SAW pressure sensor on quartz membrane lapping," *10eme Congres Francais d'Acoustique,* 2010.

[3] S. Grousset *et al.*, "SAW pressure sensor based on single-crystal quartz layer transferred on Silicon," *IEEE EFTF/IFCS,* pp. 980-983, July 2013.

[4] S. C. Moulzolf, R. Behanan, R. J. Lad, and M. P. d. Cunha, "Langasite SAW Pressure Sensor for Harsh Environments," *IEEE International Ultrasonics Symposium Proceedings,* pp. 1224-1227, 2012.

[5] P. Nicolay *et al.*, "A LN/Si-Based SAW Pressure Sensor," *Sensors,* vol. 18, no. 10, p. 3482, 2018.

[6] T. Aubert, O. Elmazria, and M. Assouar, "Wireless and batteryless surface acoustic wave sensors for high temperature environments," *Intl Conf Elec Meas & Instr,* 2009.

[7] Q. Xie *et al.*, "Effectiveness of oxide trench array as a passive temperature compensation structure in AlN-on-silicon micromechanical resonators," *Appl Phys Lett,* vol. 110, no. 8, p. 083501, 2017.

[8] T. Hoang, "Design and realization of SAW pressure sensor using Aluminum Nitride," PhD Thesis, 2009.

[9] V. Chidambaram, B. Y. Ho, and S. Gao, "Development of CMOS Compatible Bonding Material and Process for Wafer Level MEMS Packaging Application under Harsh Environment," *ICSIC 2012,* 2012.

[10] E. J. Ng, V. A. Hong, Y. Yang, C. H. Ahn, L. M. C. Everhart, and T. W. Kenny, "Temperature Dependence of the Elastic Constants of Doped Silicon," *JMEMS,* vol. 24, no. 3, pp. 730 - 741, 2015.

[11] H. J. McSkimin, "Measurement of Elastic Constants at Low Temperatures by Means of Ultrasonic Waves–Data for Silicon and Germanium Single Crystals, and for Fused Silica," *J Appl Phys,* vol. 24, no. 8, pp. 988-997, 1953.

[12] R. Farraro and R. B. McLellan, "Temperature dependence of the Young's modulus and shear modulus of pure nickel, platinum, and molybdenum," *Metallurgical Transactions A,* vol. 8, no. 10, pp. 1563-1565, 1977.

CONTACT

*E.J. Ng; eldwin_ng@ime.a-star.edu.sg